IEEE Access
Multidisciplinary | Rapid Review | Open Access Journal

Received November 16, 2018, accepted December 2, 2018, date of publication December 14, 2018,
date of current version January 7, 2019.

Digital Object Identifier 10.1109/ACCESS.2018.2887005

On Performance Analysis of Single Frequency Network With C-RAN

YEKTA TURK[1], ENGIN ZEYDAN[2], (Member, IEEE), AND CEMAL ALP AKBULUT[1]
[1]Mobile Access Systems Architecture Department, Türk Telekomünikasyon A.S., Istanbul 34889, Turkey
[2]Centre Technologic de Telecomunicacions de Catalunya, 08860 Barcelona, Spain

Corresponding author: Engin Zeydan (engin.zeydan@cttc.cat)

This work was supported in part by Spanish MINECO under Grant TEC2017-88373-R (5G-REFINE) and in part by the Generalitat de Catalunya under Grant 2017 SGR 1195.

ABSTRACT Centralized-RAN (C-RAN) is an architectural trend that uses resource sharing and a set of interference mitigation techniques to reduce capital and operational expenditures for mobile network operators (MNOs). One of the technical enablers of a C-RAN solution is single frequency network (SFN) that curbs the interference and allows MNOs to transmit over single frequency across coordinated cells. One of the main advantages of SFN is that it reduces the number of handovers between neighboring cells while improving the overall system performance. In contrast to previous approaches that demonstrate some of the most prominent C-RAN features, in this paper, we first investigate two different SFN deployment scenarios' characteristics, benefits, and limitations. Second, we perform a simulation analysis of non-SFN and SFN without joint scheduling to observe signal to interference ratio heatmap distribution of the experimental test-site using similar system configurations. Finally, we perform an experimental analysis of joint scheduling in SFN based on coordinated inter baseband units scenario using C-RAN in a realistic environment. The experimental results are tested on a real operating site of a major MNO's infrastructure in Turkey. Through experimental results, we show overall performance gains of SFN feature in terms of different key performance indicators that are obtained from coordinating remote radio units in an SFN cell. Finally, we discuss about the main takeaways, lessons learned, and challenges of the considered SFN implementation.

INDEX TERMS C-RAN, coordination, joint scheduling, SFN, experiment, testbed.

I. INTRODUCTION

Increasing, mobile data demand and scarce spectrum resources are pushing Mobile Network Operators (MNOs) to build cellular networks from a new perspective [1]. For this reason, MNOs are upgrading their mobile network infrastructure periodically almost every decade. Compared to previous 3G/4G cellular network evolution tracks that were designed mainly for telecommunication operators, vendors and end-users, 5G technology is expected to improve the whole society by connecting not only smartphones, but everything in the future. Hence, the interest in 5G networks does not only rise from MNOs and telecommunication vendors, but also from different industries and communities. Various third parties (e.g. automobile and factory industries) are interested in 5G network's capabilities and demand for its availability in near future as well.

5G standards are expected to become available late 2019 by International Telecommunication Union (ITU)-R Working Party [2]. 3GPP is following a similar timeline for 5G standardization process [3]. Early 5G commercial deployments are announced by various [4], [5]. However, there are also concerns that large-scale 5G deployments may require high level of investments by operators. For example, the latest report of ITU estimates that the cost of deployment of a 5G ready network with small cells can cost around USD 6.8 million for a small city and USD 55.5 million for a large and dense city [6]. In this report, the recommendation from ITU for operators and policy-makers is to consider 5G as an enhancement of 4G networks in terms of availability and quality. Therefore, the most of the capabilities that make 5G more effective appears to be enhanced forms of Long Term Evolution (LTE). Moreover, recent 5G standards demonstrate that 5G design should also be integrated with Long Term Evolution Advanced (LTE-A). For example, the first 5G commercial deployments using the The 3rd Generation Partnership Project (3GPP) Release 15 specification is planned to be with

non-standalone architecture. In non-standalone architecture, LTE-A network is still used for legacy network for mobility control, while gigabit data transfer is accomplished with 4G or 5G networks. Hence, initial 5G launch is expected to focus on mobile broadband experience enhancements by re-using the existing architecture, network sites and packet core.

Centralized RAN (C-RAN) architecture is identified as one of the leading candidate for 5G network deployments [7]. C-RAN architecture has brought along new approaches such as software defined networks, cloud computing and virtualization. Hence, there are several advantages of C-RAN-enabled architecture, including resource pooling, layer inter-working, scalability, load balancing between cells and facilitation of cooperative transmission and reception strategies. Spectrum efficiency can also be boosted together with cooperation between Remote Radio Units (RRUs) for interference mitigation. However, there are some problems with C-RAN deployment as well. For example, when RRUs are deployed in densely populated outdoor areas, they are spaced small distances apart to ensure coverage. This deployment model can lead to high interference between physical cells, so the control channels cannot be properly demodulated and the signal-to-interference-plus-noise ratio (SINR) of Physical Downlink Shared Channel (PDSCH) for Cell Edge Users (CEUs) decreases. Therefore, cell throughput decreases and user experience deteriorates.

To mitigate these undesirable effects, various features of LTE-A such as Carrier Aggregation (CA), Coordinated Multipoint (CoMP) and Single Frequency Network (SFN) are understudy. Among these, SFN is a significant feature of LTE-A that can enable multiple physical cells to be combined into one logical cell. This logical cell is called an SFN cell and the area served by an RRU is called a physical cell. Generally, SFN feature allows overlapping areas between physical cells to become part of the SFN cell center. SFN also provides multiple RRUs that work on the same Physical Cell ID (PCI) in a geographic area to serve as one cell. Note that PCI is one of the essential radio parameters consisting of Primary Synchronization Signal (PSS) and Secondary Synchronization Signal (SSS) and ranges from 0 to 503 [8]. PCI assignments are carefully planned by MNOs for collision and confusion free assignment with each cell's neighbors. Some benefits of SFN are mitigation of co-interference between cells via radio access network (RAN) coordination, reduction of number of handovers between neighboring cells and improvement of SINR. Under normal conditions, a single-frequency LTE network creates very high interference between cells, especially for CEUs. If SFN is used, RAN resources are shared between multiple participating cells via RAN coordination. As a result, better user experience gains can be achieved within the overlapping areas of participating physical cells especially for CEUs.

To meet the future demands of end-users effectively, next generation cellular architecture will need to promote efficient resource sharing and improved coordination between network systems during their evolutionary process. C-RAN provides attractive opportunities for MNOs including flexibility, scalability, cost reduction and rich services. SFN on the other hand, can provide reduced interference and less Handover (HO) rates between the physical cells. Hence, combining SFN in a C-RAN architecture is a promising solution for improved network efficiency for MNOs.

The rest of the paper is organized as follows: Section II gives the related works and main contributions of the paper. Section III provides architecture, system model and concepts for SFN cell building process. Section IV provides C-RAN components and site configuration for creating a SFN cell. Section V gives the simulation results for non-SFN and SFN without joint scheduling and experimental results for *Joint scheduling in SFN based on coordinated inter-BBU* and non-SFN activation periods in C-RAN. Finally, Section VI provides the conclusions.

II. RELATED WORKS AND MAIN CONTRIBUTIONS

In recent studies, little research efforts have been developed for practical demonstrations of the capabilities of SFN framework in C-RAN. Most of the previous approaches in the literature on SFN have focused on broadcast services in LTE/5G networks [9]–[12]. SFN is first used as an Evolved Multimedia Broadcast Multicast Services (eMBMS) feature where same data is transmitted (over OFDM symbol level) by clustered eNodeBs over a common set of time-frequency resources. LTE's broadcast service named as Multimedia Broadcast Single Frequency Network (MBSFN) is introduced in LTE Release 9 where same content is broadcast to all or group of users in a cell using a subset of available resources. The aim is to increase SINR for CEUs. The interference among eNodeBs becomes constructive through this synchronous transmissions and same signals are combined at user equipments (UEs) to enhance received SINR. Sivaraj *et al.* [9] study SFN clustering and resource allocation using NS3 simulations. The paper has shown up to 40% broadcast/unicast performance improvements with a prototype named BoLTE in a C-RAN testbed. Clustering of eNodeBs based on similarity of content between applications and SFN area formation are considered in [11]. Rinalid *et al.* [12] aim to maximize aggregate system throughput via a formation algorithm in MBSFN areas over 5G Networks. Challenges and future directions of eMBMS over future 5G systems are detailed in [13]. For delivery of identical contents to a group of users in a scenario similar to eMBMS, Montalban *et al.* [14] propose joint use of subgrouping multicast techniques and non-orthogonal multiple access (NOMA). SFN transmission of both data and control signals for mobility robustness and higher CEU throughput are shown in [15]. SFN in unlicensed spectrum deployment solutions for delivery of common media content to large number of users are investigated in [16]. Besides, in the literature there are not many various works on SFN implementation scenarios. NTT Docomo (Japan) has recently published an article describing 3GPP's Release 14 specifications on a SFN scenario for high speed moving mobile environments to

improve mobile communications quality [17], [18]. In these works, a SFN scenario is studied to improve Physical Random Access Channel (PRACH) detection performance in high-speed mobile environments.

Coordination between cells is going to be more important to maximize user experience and increase spectrum efficiency. In general, cell coordination can be done for different purposes such as mobility management (handover), traffic and interference management, joint transmission and reception, carrier aggregation and dual connectivity [19]. The classical approaches on scheduling are mostly based on association of UEs to Base Stations (BSs) [20]–[22]. The paper in [20] studies a coordinated scheduling method among BSs in LTE Downlink (DL) to avoid inter-cell interference. Using coordinated scheduling with cell clustering, Nardini *et al.* [21] show how network performance can be improved in terms of protecting CEUs from interference while using fewer resources. A coordinated scheduling problem for the DL of C-RAN to maximize the network utility with an heuristic interference-aware greedy algorithm is studied in [22]. A RAN sharing scheduling mechanism among MNOs in a given C-RAN architecture is given in [23]. Douik *et al.* [24] propose a coordinated scheduling technique using a graph theoretical approach for DL of C-RAN.

Similarly, C-RAN implementations are abundant in industry and MNOs [25], [26] since its first introduction by China Mobile [27]. A thorough survey of C-RAN trials and testbeds with key technologies and architectures in C-RAN is given in [28]. China Mobile's field trials have demonstrated throughput gains up to 300% in Uplink (UL) [25]. The white paper in [19] analyzes different architecture options of C-RAN and points out their fundamental benefits and challenges. C-RAN related technological definitions (e.g. CA, CoMP, SFN) are provided in state-of-art analysis work of Checko *et al.* [26]. Various works showing the benefits of CA and CoMP in C-RAN is shown in simulations and experimental evaluations in [25], [29], and [30].

A related interference mitigation technique of CoMP transmission/reception (Tx/Rx) has been proposed in 3GPP's LTE Release 9 with two main categories of CoMP schemes: Joint Processing (JP) and Coordinated Scheduling (CS). Both JP and CS have their advantages and disadvantages where JP's throughput gains may be larger than CS but has higher complexity than CS due to data availability requirement at the coordinating cells [31]. The impact of gathering more eNodeBs into the CoMP set for realizing the Joint Transmission (JT) CoMP in C-RAN in simulations is investigated in [32]. The paper in [33] investigates the impact of X2 link failures on the performance of different JT-CoMP scenarios using a traditional LTE-A network. The effect of CoMP-JT on UE's DL throughput using field trials is studied in [34]. A quality-of-service (QoS) priority-based CS and hybrid spectrum scheme for DL CoMP transmission is studied in [31]. According to 3GPP TR 36.819 v11.2.0 (2013-09) [35], four different CoMP scenarios were proposed where CoMP can be beneficial. In CoMP scenario 4 of [35], CoMP is between a macro cell and multiple low transmit power Remote Radio Head (RRH) where Tx/Rx points created by RRH have same Cell-ID as the macro cell's ID. This scenario is an example application of SFN jointly with CoMP.

Our Contributions: As evidenced by prior art on this topic, the above state-of-the-art papers utilize the SFN and C-RAN separately and do not leverage the benefits of mixed strategies, along with the general tendency to omit the challenges of real-world implementations while targeting different deployment strategies. Further, early studies considered C-RAN implementations with some of its prominent features including CA, CoMP Tx/Rx accounting for limited number of Key Performance Indicators (KPIs). No prior efforts have concentrated on C-RAN test-bed implementation results of SFN feature together with different deployment scenarios. Therefore, it is imperative to account the performance of different KPIs and Physical Resource Block (PRB) utilization ratios for the overall performance improvements while working on practical environments with more realistic assumptions. This paper addresses the real-world implementation of SFN feature in an operational C-RAN platform. Since SFN in C-RAN itself is a new technology, to the best of our knowledge, no experimental C-RAN platforms have been built to show the benefits of C-RAN supporting SFN cell in real-world operational networks. Main contributions of this paper can be summarized as follows:

- We use an experimental C-RAN platform to fully exploit the benefits of joint Tx/Rx scheduling strategy with SFN based on coordinated inter-Baseband Unit (BBU) design framework, with two configurations of the system in which one of them is implementing *Joint scheduling in SFN (J-SFN) based on coordinated inter-BBU and the other is non-SFN configuration scenario*.
- We provide insights on the benefits and limitations of different SFN scenarios and evaluate the impact of SFN on different observed KPIs of evolved Node-B (eNodeB) for 14 days in an operational network site in Istanbul, Turkey.
- We provide simulation results for non-SFN and SFN without joint scheduling methodologies to observe the SINR heatmap distribution over the considered experimental region of interest under similar configurations.
- Our experimental results indicate that *Joint scheduling in SFN (J-SFN) based on coordinated inter-BBU* yields improvements on some KPIs (e.g. Channel Quality Indicator (CQI) and Modulation Coding Scheme (MCS)) compared to non-SFN sites whereas the improvements are slim in some other KPIs (including DL/UL throughput) due to observed trade-off between the effect of joint Tx/Rx and large ratio of average number of jointly scheduled UEs to all LTE UEs in the considered SFN cell.

III. ARCHITECTURE, SYSTEM MODEL AND CONCEPTS

Consider a jointly coordinated Tx/Rx scheduling in a SFN within a C-RAN. SFN consists of R RRUs, indexed by

$\mathcal{R} = \{1, \ldots, R\}$ connected to a central BBU pool in a central processing location cooperatively serving U different UEs in total, indexed by $\mathcal{U} = \{1, \ldots, U\}$ in a given SFN cell over a shared spectrum with bandwidth w and B Resource Blocks (RBs), indexed by $\mathcal{B} = \{1, \ldots, B\}$. Each RRU is assumed to have N_t transmit antennas and each UE to have N_r receive antennas. A central BBU pool coordinates all joint Tx/Rx scheduling strategy of RRUs (as well as synchronization of all transmit/receive frames) and scheduling strategies of UEs. Let the time horizon be divided into discrete time slots (days in this paper) and indexed as $\mathcal{T} = \{1, \ldots, T\}$. At each time slot $t \in \mathcal{T}$, many UEs are scheduled to transmit/receive to/from their cooperative RRUs. The front-haul communication link between BSs and BBU are used to communicate the scheduling information. The throughput of UL or DL transmission is dependent on the received SINR.

Consider a DL in a cellular system with a total of M number of RRUs operating in a large region with each RRU operating under same frequency. R is the total number of the cooperating RRUs in an SFN cooperating set. Each sector has R RRUs out of the total M RRUs to perform joint scheduling based on SFN with coordinated inter-BBU. Hence, the SFN user $u \in \mathcal{U}$ will be scheduled to receive the same data x_u from R cooperating RRUs, while $(M - R)$ RRUs will cause the interference. Thus, the signal received by a user $u \in \mathcal{U}$ from R cooperating RRUs after SFN is activated can be written as

$$y_u = \sum_{r=1}^{R} H_{u,r} W_r x_u + \sum_{m=R+1}^{M} H_{u,m} W_m x_m + n_u \qquad (1)$$

where $\boldsymbol{H}$ is the channel matrix, $\boldsymbol{W}$ is the precoding matrix to cancel the interference, x is the data symbol and n_u is additive white Gaussian noise. Therefore, $(M-R)$ RRUs are operating in an uncoordinated way. Hence, the received power from $(M-R)$ RRUs will be treated as interference to the SFN users. The SINR at user $u \in \mathcal{U}$ using joint SFN based on coordinated inter-BBU is

$$SINR_u^b = \frac{\sum_{r=1}^{R} |H_{u,r} W_r|^2 P_{u,r}^b}{\sum_{m=R+1}^{M} P_{u,m}^b |H_{u,m} W_m|^2 + \sigma^2} \qquad (2)$$

where $P_{u,r}^b$ is the transmitted power from RRU $r \in \mathcal{R}$ at RB $b \in \mathcal{B}$ and σ^2 is the noise power. For simulation purposes, we have used an empirical path loss model named as Standard Propagation Model (SPM). SPM is used for path loss prediction and is an extended version of Hata path loss formula [36]. The received signal can be expressed as,

$$\begin{aligned} P_r = P_t - \{&K_1 + K_2 log(d) + K_3 log(h_t) \\ &+ K_4 DiffractionLoss + K_5 log(d) log(h_t) + K_6 h_r \\ &+ K_7 log(h_r) + K_{clutter} f_{clutter} + K_{hill}\} \end{aligned} \qquad (3)$$

where P_r is the received power of incoming desired signal, P_t is the transmit power (EIRP) (dBm), K_1 is a constant offset (dBm), K_2, K_3, K_4, K_5, K_6, K_7 and $K_{clutter}$ are multiplication factors chosen based on MNOs' optimization policies, Diffraction Loss (DiffractionLoss) is loss due to diffraction over obscured path, h_r is effective mobile receiver antenna height (m), $f_{clutter}$ is the average of weighted losses due to clutter and K_{hill} is the corrective factor for hilly regions.

In comparison to normal cellular C-RAN enabled sites, RRUs send/receive the same signal to/from UEs simultaneously under the same frequency in an SFN scenario. In SFN, there exists a master and slave stations. SFN is especially suitable for scenarios when there is no interference from neighbor RRUs, so less handovers occur in case of UEs mobility. The difference between non-SFN and SFN cells is given in Fig. 1.

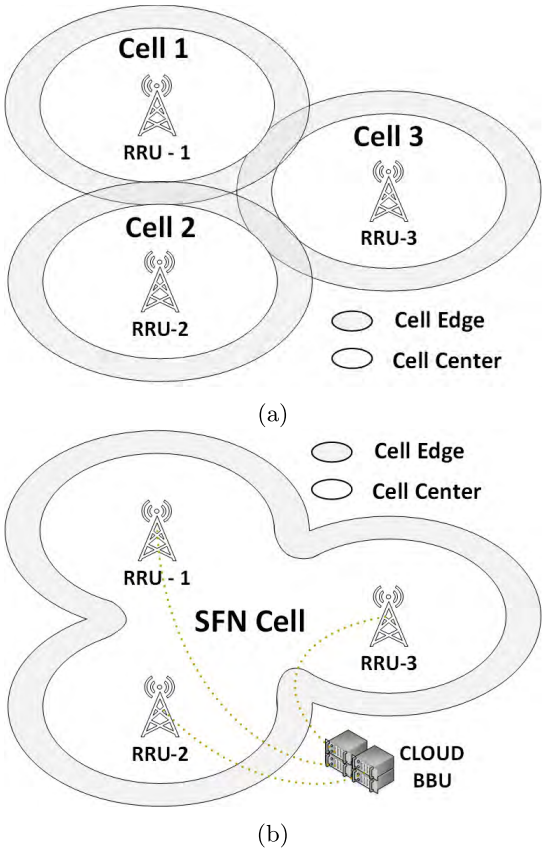

FIGURE 1. (a) Non-SFN cells (b) SFN cell.

For outdoor coverage scenarios in which RRUs are placed together in densely populated areas, high interference among physical cells can emerge due to small distances. This can decrease the SINR of PDSCH for CEUs as well as deteriorate control channel's demodulation capabilities. Therefore, the cell throughput and user experience also deteriorate. Together with C-RAN's SFN feature, multiple cells can be combined to prevent handover over those combined cells as shown in Fig 2. In the case that SFN is utilized inside a cluster of cells, normal UEs that are in cell-edge become part of the SFN cell center. This effect reduces both the interference and the number of handovers within cells.

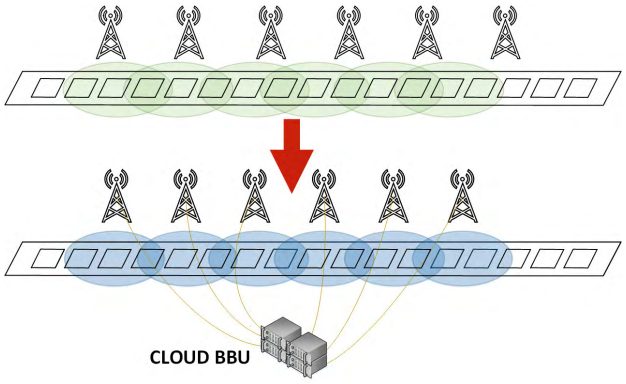

FIGURE 2. Cell combination with SFN.

A. JOINT COORDINATED AND INDEPENDENT TRANSMISSION/RECEPTION FOR UL AND DL

Fig. 3 gives two examples of joint coordinated and independent Tx/Rx methods. In joint coordinated Tx/Rx, multiple RRUs transmit/receive the same data to/from the same UE whereas in independent Tx/Rx, only one RRU is selected

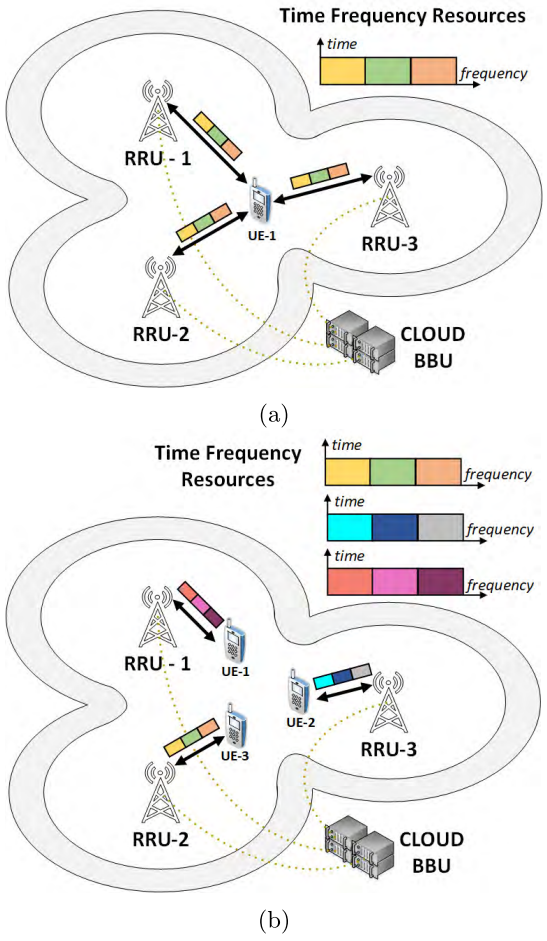

FIGURE 3. (a) Joint transmission/reception with RRUs. (b) Independent transmission/reception with RRUs.

to be transmitting (receiving) same data to (from) a UE in an SFN cell. Fig. 3a shows an example of joint coordinated Tx/Rx method when RRUs are used. Fig. 3b, on the other hand, displays an example of independent Tx/Rx method. In this case, using the same time-frequency resources, different RRUs can simultaneously Tx/Rx different data to/from different UEs.

One of the main challenges of SFN design in LTE networks is to manage *the diversity-multiplexing trade-off* [9]. For example, when clustering RRUs together in an SFN cell, there exists a risk that an individual RRU's data rate in the cluster can be decreased. This may limit some individual RRU's effective multiplexing of traffic over their resources. Hence in such cases, it is better to schedule UEs in this RRU independently. To recognize whether a UE occupies the time-frequency resources of one or more RRUs, *independently scheduled UE* and *jointly scheduled UE* terms are introduced in both UL and DL directions. When UE occupies the time-frequency resources of multiple RRUs, this UE is called a *jointly scheduled UE*. During joint transmission in an SFN cell, no interference occurs between RRUs' physical channels, i.e. on Physical Downlink Common Channel (PDCCH) and PDSCH. Moreover, this ensures higher SINR for CEUs in physical channels. When UE occupies time-frequency resources of only one RRU, this UE is called an *independently scheduled UE*. In this case, eNodeB allocates a set of dedicated transmission resources to serve each independently scheduled UEs.

Table 1 summarizes pros and cons of utilizing *joint coordinated* and *independent Tx/Rx* in an SFN cell. The unique characteristic of *joint scheduling* in an SFN cell is that eNodeB always performs joint scheduling, regardless of the position of the UE. Joint scheduling is more useful when there is low load (and generated throughput) on SFN sites and the mobility between the considered SFN sites is high. Low PRB utilization requirement is due to fact that joint scheduling also increases PRB utilization ratio. Additionally, interference prevention is more efficient in outdoor environment for joint scheduling in an SFN cell. Hence, if there are small number of UEs and a light traffic load (e.g. less than 30% utilization of RBs), SFN can reduce the number of handovers when RRUs are deployed in urban outdoor areas. For this reason, SFN is mainly useful in scenarios when there exists high frequency of handovers between cells, e.g. in railways with the aim to provide zero handovers. There exists limitations of joint scheduling as well. For example, it can not be used in conditions with high PRB utilization because it increases PRB utilization inside the cells.

In *independent scheduling*, RRUs will schedule UEs based on their proximity. It is more suitable for indoor areas when there is coverage for all RRUs. Additionally, it can schedule more UEs per given Transmission Time Interval (TTI). Some of the limitations of independent scheduling are as follows: First, it needs UE support for better channel estimation and Transmission Modes (TMs) 9-10 should be enabled for both UE and eNodeB. Second, this scheduling is not effective

TABLE 1. Characteristics, limitations, operation & benefits of SFN transmission/reception techniques.

SFN Tx/Rx Technique	Characteristics	Operation & Benefits	Limitations
Joint Scheduling	eNodeB always performs joint scheduling, regardless of the position of the UE.	i) More plausible when there is low load (and generated throughput) on the site. ii) Ideal when the mobility ratio in the site is high. iii) Interference prevention is more efficient in outdoor environment.	It can not be used in places with high PRB usage because it increases PRB utilization.
Independent Scheduling	UE's proximity to RRUs is calculated. RRU that will schedule UE is decided later.	i) It can schedule more UE per given TTI. ii) It is more suitable for indoor areas where there is coverage for all RRUs.	i) UE support is required for better performance (TM-9, TM-10). ii) It is not effective when mobility is high. iii) In low load sites, there is possibility of negative effect caused by the inconsistency between CRS SINR and PDSCH SINR.

when there is high UE mobility inside SFN cell. Third, during low load scenarios there is a possible negative effect caused by the inconsistency between Cell Reference Signal (CRS) SINR and PDSCH SINR. Configuration of eNodeB with TMs 9-10 and usage of this mode by UE eliminate this drawback due to UE dedicated reference signal besides CRS.

Scheduling Methodology: In the following analysis, our experimental efforts are especially focusing on cooperative joint Tx/Rx scheduling strategy in C-RAN. Compared to CS, joint scheduling can provide higher throughput gains however can suffer from high implementation complexity [31]. This is due to the joint scheduling requirement. The frames in joint scheduling are allocated to UEs under same E-UTRA Absolute Radio Frequency Channel Number (EARFCN), same TTI when same data is transmitted in all the cooperating cells of the SFN. Therefore, both UE data and scheduling decisions are shared among the cooperative cells to minimize the interference among UEs. This can make the scheme unsuitable for SFN in case of nonideal backhaul existence. Due to transmit diversity vs. resource multiplexing trade-off in SFNs [9], a balance is also required between joint and independent scheduling in a SFN cell. Therefore, C-RAN design should consider this trade-off. However, joint coordinated and independent scheduling implementation comparisons for remote RRU users are left for future research work.

B. JOINT SCHEDULING IN SFN (J-SFN) BASED ON COORDINATED INTER-BBU

If SFN is performed over multiple BBUs, then it is named as inter-BBU SFN. During application of SFN based on inter-BBU coordination, we compare non-SFN scenario (with normal macro sites) with *J-SFN based on coordinated inter-BBU* implementation.

1) J-SFN BASED ON COORDINATED INTER-BBU

enables multiple RRUs to serve to only one SFN cell. Joint scheduling of RRUs is adapted within SFN cell by inter coordination of BBUs inside C-RAN. For UL, one or multiple RRUs are selected by SFN cell to receive signals jointly or independently from single UE on UL physical channels. In the DL, multiple RRUs are used for joint transmission of signals into UE on DL physical channels. Together with J-SFN feature, signals that are mutually interfering from different cells are transformed into enhanced multiple signals that are arriving from a single SFN cell. The aim is to increase the SINR for CEUs and to reduce inter-cell interference due to decreased number of neighboring cells. Hence, the user experience at cell-edge can be improved.

2) AN EXAMPLE OF JOINT RESOURCE SCHEDULING

Fig. 4 shows an example scenario for application of joint scheduling to different UEs. The eNodeBs adopt joint scheduling to allocate resources to a UE. UEs that are in the overlapping area such as UE-1, UE-2 and UE-3 are eligible

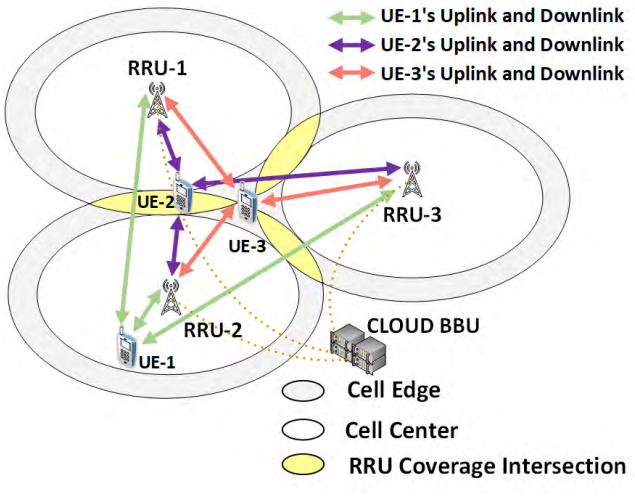

FIGURE 4. Joint resource scheduling is applied by eNodebs to all UEs inside SFN cell.

FIGURE 5. BBU pool used in TT central office location of C-RAN in Cekmekoy district of Istanbul.

for *joint scheduling* by eNodeB in Fig. 4. All UEs are receiving same signals from multiple RRUs (RRU-1, RRU-2 and RRU-3 namely) simultaneously. Therefore, if a UE is on the coverage area of multiple RRUs, then same data is scheduled to be transmitted/received to/from UE in DL/UL. In the next sections, we first start to investigate C-RAN components and site configurations for successful SFN activation and later present SFN experimental and simulation evaluations and results.

IV. C-RAN COMPONENTS AND SITE CONFIGURATIONS FOR SFN CELL

The C-RAN implementation architecture is shown in Fig. 6. For experimental trials, we have used commercial Evolved Packet Core (EPC) and eNodeBs together with test and real UEs in live network. For SFN, new RF plans are deployed to convert sites to an SFN cell. Each sector requires one Common Public Radio Interface (CPRI) connection whose capacity is highly dependent on Multiple Input Multiple Output (MIMO) and bandwidth configurations. CPRI link is carried over Dense Wavelength Division Multiplexing (DWDM) equipments that are installed in each site and in the central office. Four sites are chosen from Cekmekoy district in Istanbul. Moreover, all sites are connected to a centralized location in Cekmekoy district for C-RAN via fronthaul connection. All LTE-A sites are centralized in this BBU pool. Fig. 5 shows the BBU pool used in central location of C-RAN. Inside C-RAN center location, the installed equipment are: four $\times$ BBUs for four trial sites, one switch for controlling C-RAN coordination features, one Optical Service Network (OSN) equipment for DWDM transmission. For remote sites, one OSN equipment for each 3 sites (*WIS*2038, *WIS*3133, *WIS*2430), and two OSN equipments for other site (*WIS*4087*A*) are used. Switch that is used for controlling C-RAN coordination features is called Controlling Switching Element (CSE) and is one of the main equipment used for BBU coordination. CSE is also used to connect different BBUs, so that RRUs connected to BBUs can be combined to serve an SFN cell. The equipment used in trial experiments can support up to 60 BBUs. LTE-A features for SFN are deployed over this controlling switch. A global positioning system (GPS) antenna is connected to the switch due to tight time synchronization requirements for BBU coordination. Both sites are synchronized via CSE. GPS is used for clock and frame synchronization of RRUs. Our C-RAN implementation for LTE eNodeB is using Frequency-Division Duplex (FDD). Therefore, reduction of co-channel interference are for both control and data channels.

Site connection plan from RRU to backhaul connection for one of four sites is given in Fig. 7. Red dashed circled area (1.0353 km^2) represents the C-RAN trial sites (for SFN cell) and purple circled areas (2.99 km^2) represent the neighboring sites of the C-RAN trial sites (Tier 1 sites). Blue colored cells represent 1800 Mhz, whereas orange colored cells represent 900 Mhz sites. Additionally, sites starting with letter "W" and "U" represent 4G and 3G sites respectively. No 3G sites are inside the experimental test side marked with red dashed circled area. The distances to TT central office of radio sites *WIS*2038 and *WIS*4087 are 0.96 km and 0.93 km respectively. The distance between *WIS*2038 and *WIS*4087 sites is 0.38 km. In case that physical cells are merged into a single SFN cell, the difference between their coverage radii becomes important. If this radii is greater than some value (e.g. 1 km in a practical systems), there exists large delays in received signals from different physical cells. In such a case, the DL performance can deteriorate due to power difference between signals arriving from different physical cells. Tier-1 site *WIS*4956 is co-located with TT central office. We collect daily averaged values of KPIs after activation of *J-SFN based on coordinated BBU*.

For evaluating the performance of SFN in C-RAN, we deployed and tested SFN feature in Cekmekoy suburban district of Istanbul Turkey as shown in Fig. 7. All the measurements are obtained from two selected sites of SFN cell, namely, *WIS*2038*A* and *WIS*4087*A* each with bandwidth $w = 20$ *Mhz* (the selection process is detailed in later subsections). Each site (*WIS*2038 and *WIS*4087) has three sectors and a total of R = 6 RRUs. There are one RRU with EARFCN = 1450 (LTE 1800 Mhz cells) and one RRU with EARFCN = 6200 (LTE 800 Mhz cells) in each cell of a single sector. Considering the fact that there are two cells (on 800 Mhz and 1800 Mhz) in a given sector, each cell has one RRU. SFN is applied between one cell of two sites *WIS*2038*A* and *WIS*4087*A* running EARFCN = 1450 RRU. The DWDM equipment in TT central office is connected to two cloud BBUs positioned separately for each site. DWDM and BBUs have a separate physical link for each RRU. A CSE is located to provide coordination between BBUs and is responsible for the synchronization of BBUs to work together.

All 3GPP compliant parameters that are used in simulations and experiments for SFN and non-SFN enabled eNodeBs are summarized in Table 2. For configuring

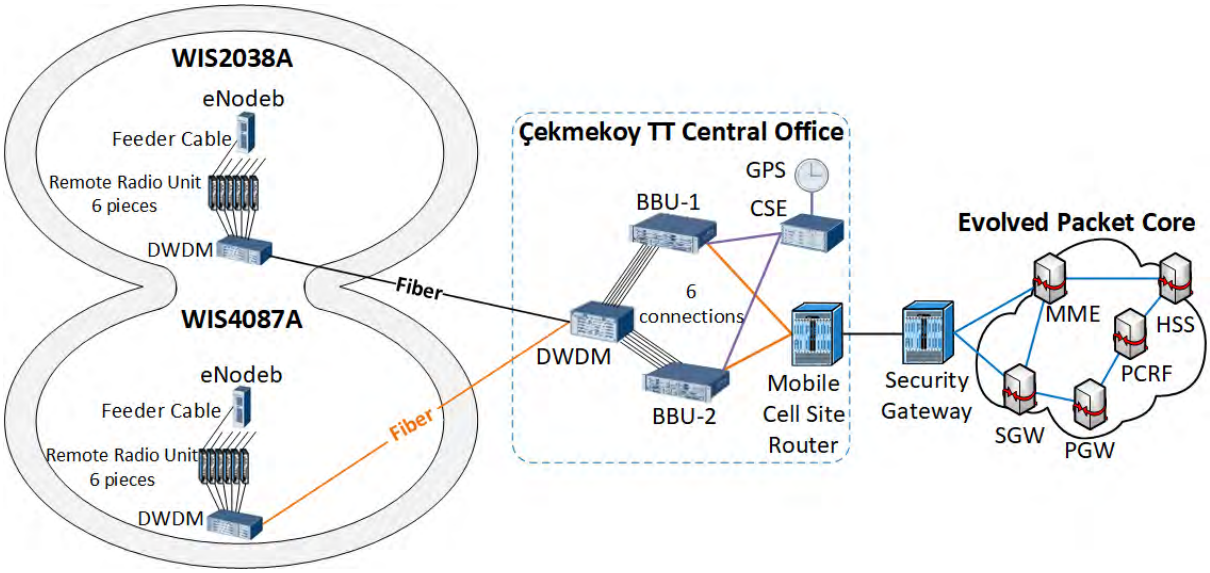

FIGURE 6. Experimental test architecture used for experimental SFN in C-RAN in Cekmekoy district in Istanbul Turkey.

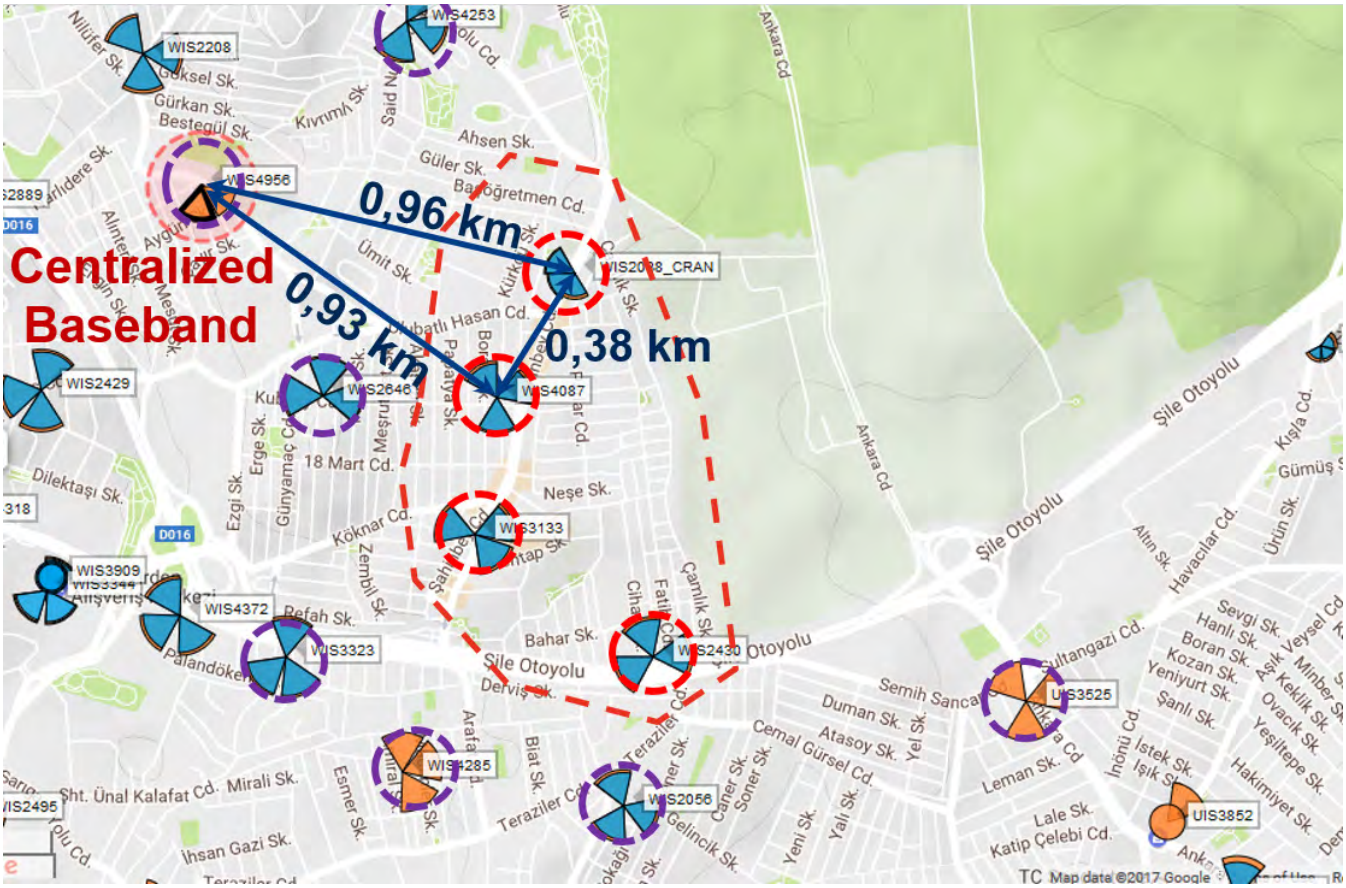

FIGURE 7. Site distribution of the experimental test site located in Cekmekoy district in Istanbul Turkey.

frequency bands, LTE specific parameters including system (channel) bandwidth, carrier frequency, adjacent channel suppression factor (used to determine adjacent interference level), sampling frequency (based on 3GPP requirement, e.g. 20 Mhz channel has a sampling frequency of 30.72 Mhz) are used.

TABLE 2. Simulation and experimental system parameters.

Parameter	Description	
Cells	WIS2038A	WIS4087A
RRU Antenna Height (eNB)	20.5 (m)	21(m)
eNB Max Power	46 dBm	
UE Antenna Height (sim.)	1.5(m)	
Number of Antennas (eNB)	1	
Traffic Model (sim.)	FTP (File Transfer Protocol)	
Cell Edge Coverage Prob. (sim.)	%88	
Number of Antennas	1	
Azimuth Angle	180^o	70^o

Parameter	Description
Carrier Frequency	1800 Mhz
System Bandwidth	20 Mhz
eNB Antenna Gain	17.32 dBi
LTE Duplex Mode	FDD
Azimuth Beamwidth	63
UE Speed (sim.)	3 km/h
Diffraction Calculation Method	Epstein-Peterson (3 obstacles)
Antenna Pattern	X Polarization
Min. RSRP (Reference Signals Received Power)	-130 (dBm)

Parameter	Description
Sampling Freq. (sim.)	30.72 (Mhz)
Adjacent Channel Suppression Factor (sim.)	25.23 (dB)
Traffic Load (DL) (sim.)	%10
PDSCH Power (avg)	45.8 (dBm)
PDCCH Power (avg)	45.4 (dBm)
Path Loss Model (sim.)	Urban, SPM (eNB)
Thermal Noise (sim.)	-104.43 dB
MIMO Mode	2 x 2
—	—

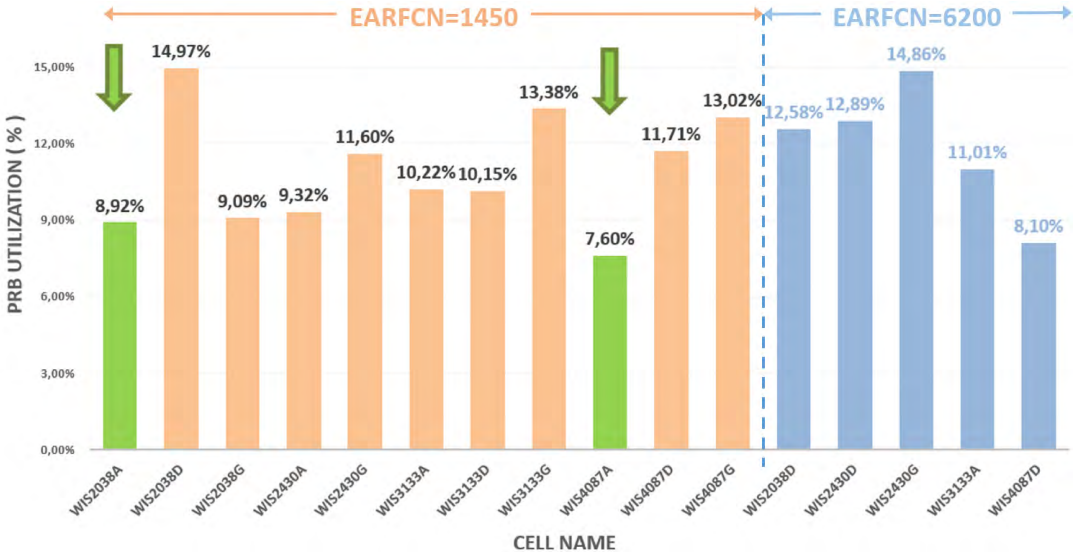

FIGURE 8. Cell PRB analysis of candidate cells for SFN cell formation process.

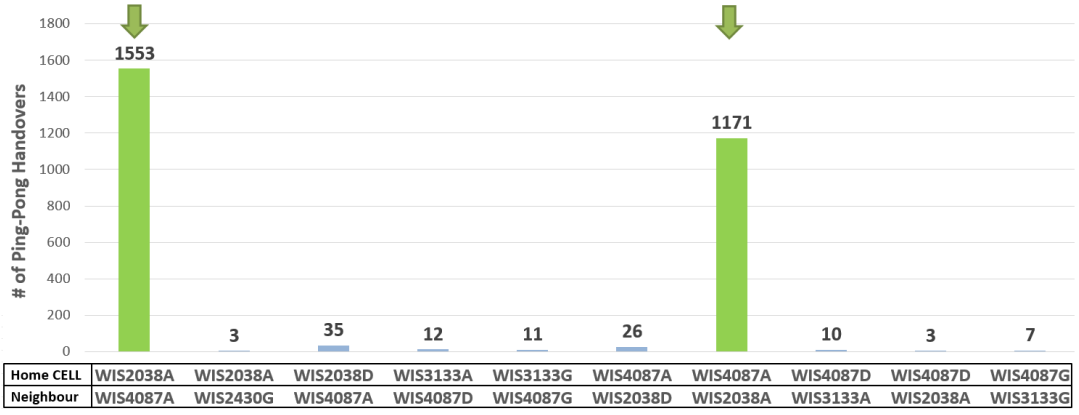

FIGURE 9. Handover attempts between neighbor sites for user behavior analysis over the candidate SFN cells.

Our experiments for monitoring and comparing *J-SFN based on coordinated inter-BBU* and non-SFN enabled sites were performed between 21 March 2017 and 03 April 2017 (i.e. for T = 14 days). *J-SFN based on coordinated inter-BBU* feature is activated between 28 March 2017 and 03 April 2017 (7 days) and non-SFN duration is between 21 March 2017 to

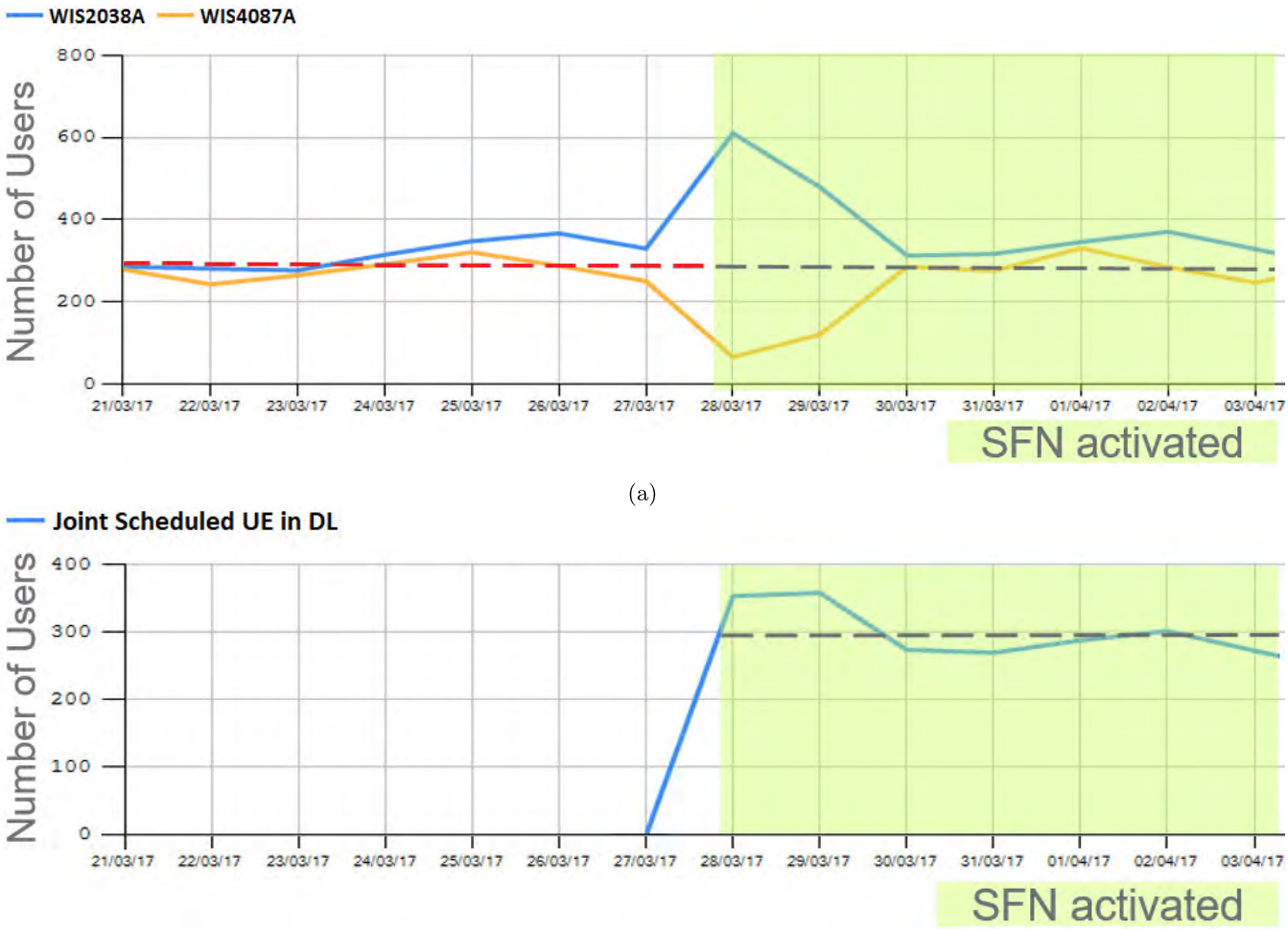

FIGURE 10. Single frequency network (a) Total number of LTE users. (b) Average number of jointly-scheduled UEs in UL.

27 March 2017 (7 days). For fair comparisons, supported functions and environment are kept the same during SFN activation and non-SFN activation observation durations. Note that the granularity of comparisons is done daily-based due to sheer volume of data that needs to be kept inside the performance optimization tools as well as better visibility of performance improvements from MNOs' operational point of view.

V. SIMULATION AND FIELD EXPERIMENT RESULTS

This section shows the performances of *J-SFN based on coordinated inter-BBU* and non-SFN enabled sites. The main objective of field trial is to measure the relative performance gains of non-SFN and *J-SFN based on coordinated inter-BBU* activation periods. Field trial results are important to investigate the achievable performances under real conditions and with real equipment limitations. Therefore, the results are more expected to be more realistic than pure simulations. On the other hand, simulation results can provide complementary insights for some conclusions that are otherwise costly operations during experiments. In our simulation analysis, we have run SINR heatmap analysis of non-SFN and SFN without joint-coordinated scheduling to inspect their effect on coverage and signal levels on different areas of the considered experimental test-site. The considered scenario is given in Fig. 7 and the experimental analysis is performed over different observed KPIs.

A. PRB UTILIZATION EXPERIMENTS FOR CELLS SELECTION OF SFN

To observe the effect of performance improvements of SFN cell, PRB DL utilization ratios of participating selected cells are selected to be low. This is due to the expected increase in PRB utilization ratios after activation of SFN cell and not to reach the backhaul capacity-limitations as a network optimization objective. In the following analysis, we observe PRB utilization ratios of some of the neighboring sites and select candidate cells. We build our SFN cluster formation strategy based on data analysis over PRB utilization ratios and handover attempts using

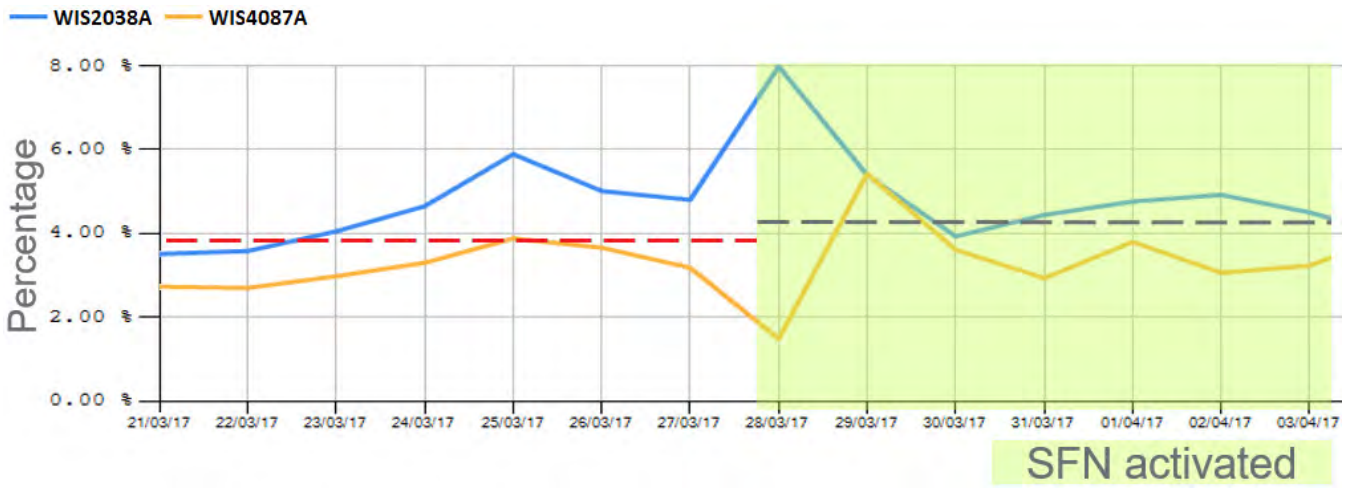

(a)

(b)

FIGURE 11. Single frequency network (a) DL utilized PRB ratio (%). (b) UL utilized PRB ratio (%).

the cell-level KPIs. The considered sites are *WIS*2038 (with cells *WIS*2038*A*, *WIS*2038*G*, *WIS*2038*D*), *WIS*2430 (with cells *WIS*2430*A* and *WIS*2038*G*), *WIS*4087 (with cells *WIS*4087*A*, *WIS*4087*G*, *WIS*4087*D*) and *WIS*3133 (with cells *WIS*3133*A*, *WIS*3133*G*, *WIS*3133*D*) as observed in Fig. 7.

Fig. 8 shows the PRB utilization analysis results for the purpose of selecting the most feasible cells in a SFN cell. Among all those considered four eNodeB sites/cells inside red circle of Fig. 7, hourly KPI values are taken on 21 February 2017. The selected cells that are suitable for SFN are those cells with busy hour PRB utilization ratio less than 15%. Fig. 8 shows cell based PRB ratios of the candidate cells for SFN cluster formation process. In Fig. 8, green and pink colored cells are cells with DL EARFCN = 1450 whereas blue colored ones are cells with DL EARFCN = 6200. From our analysis, we have selected to use cells with DL EARFCN = 1450 mainly due to two reasons: (i) cells' PRB utilization ratios with DL EARFCN = 1450 are less than the other cells with DL EARFCN = 6200 and (ii) number of cells with DL EARFCN = 1450 is higher than other EARFCN cells due to MNO's investment policy over 1800 Mhz band. After analysis of DL EARFCN = 1450 cells, *WIS*2038*A* and *WIS*4087*A* are among the top two candidate cells in SFN (also marked with green arrows on top of Fig. 8) with the lowest PRB utilization ratios of 8.92% and 7.60% respectively.

In addition to above PRB based analysis, we perform another analysis to determine cell selections inside SFN cluster. Using the inter-cell handover attempts data of 21st February 2017, we analyze LTE cell users daily inter-cell handover activities between the above selected cells and their neighbors. Fig. 9 shows the number of handover attempts between home cells and their neighbor cells. The highest number of ping-pong handover attempts occurs between the cells *WIS*2038*A* and *WIS*4087*A* with 1553 outgoing and 1171 in-going number of HO attempts respectively which are also marked with green arrows on top of Fig. 9.

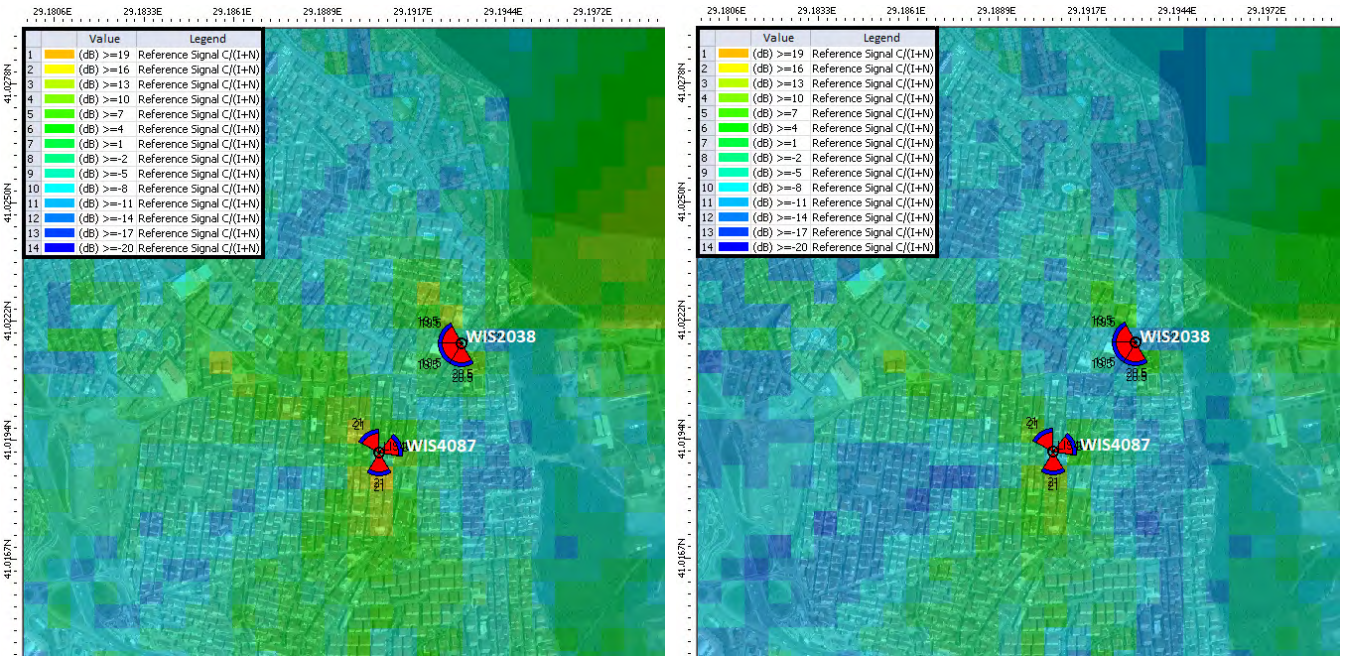

(a) (b)

FIGURE 12. Simulated heat-map of DL SINR calculated by reference signal for selected eNodeBs (a) Cells are in non-SFN mode. (b) Cells are running in SFN without joint scheduling. [Figure is best viewed in colors].

In summary, based on low PRB utilization ratios and large HO-in and out attempts between cells, green colored cells in Fig. 8 and Fig. 9 (namely *WIS*2038*A* and *WIS*4087*A*) are selected as candidate cells to increase the effectiveness of SFN cell. Generally, there are many ping-pong handovers between these two cells compared to others. Since SFN will lead to high PRB utilization ratios, it is appropriate to select these two cells with low PRB utilization ratios as well.

B. SIMULATION ANALYSIS

In this section, we perform simulation analysis of the considered non-SFN and SFN without joint scheduling scenarios using Atoll RF Network Planning tool [37]. For SFN scenario without joint coordinated scheduling, we have utilized SFN configurations where each BS is utilizing Proportional Fair (PF) scheduling without inter-site coordination, hence high interference scenario is created due to utilization of same EARFCN and PCI in both cells inside SFN cell. For cells in non-SFN mode, same EARFCN with different PCI values are configured which is similar to experimental live network configuration. The simulation parameters that are used to obtain these figures are summarized in Table 2. Note that channel parameters of K_1 to K_7 in (3) are operator specific and determined by MNOs based on their optimization and planing process. Therefore, without loss of generality, their values are omitted for privacy reasons. Moreover, no hilly-terrain topological conditions and no clutter are assumed in the considered experimented site (i.e. $K_{hill} = 0$ and $K_{clutter} = 0$). Diffraction loss is calculated using Epstein-Peterson model with 3 obstacles [38]. The simulation parameters are selected to be similar to parameters used in experimental results' conditions. We use simulations to generate SINR heatmaps to observe the effect of non-SFN and SFN without joint scheduling methodologies. In general, obtaining SINR heatmap of the region of interest can be costly in real-experimental sites due to the requirements for real-hardware and dedicated operational units. However, with simulations network behavior can be understood better via large-scale simulations. Fig. 12 shows the simulation results of the SINR heatmap for the selected cells, i.e. for *WIS*2038*A* and *WIS*4087*A*. We have used CRS SINR as our reference values to build the SINR heatmaps of Fig. 12. Fig. 12a shows heatmap when cells are in non-SFN mode whereas Fig. 12b shows the case when two cells are in SFN without joint scheduling mode. Comparing Fig. 12a and Fig. 12b, we can observe that blue colored areas (low SINR regions) are larger in Fig. 12b and better SINR distributions are observed in non-SFN mode. Therefore, the results in Fig. 12b indicate that if the cells inside SFN are not jointly scheduled by C-RAN, SFN can create an enormous amount of interference which can severely degrade the communication activity in the considered coverage areas.

C. EXPERIMENTAL SFN KPI PERFORMANCES

To evaluate the impact of C-RAN features, we have performed system performance comparisons with extensive test cases over UL-DL throughput and PRB utilization ratios, DL Packet Data Convergence Protocol (PDCP) volume, MCS, CQI, Radio Resource Control (RRC) set-up success/service

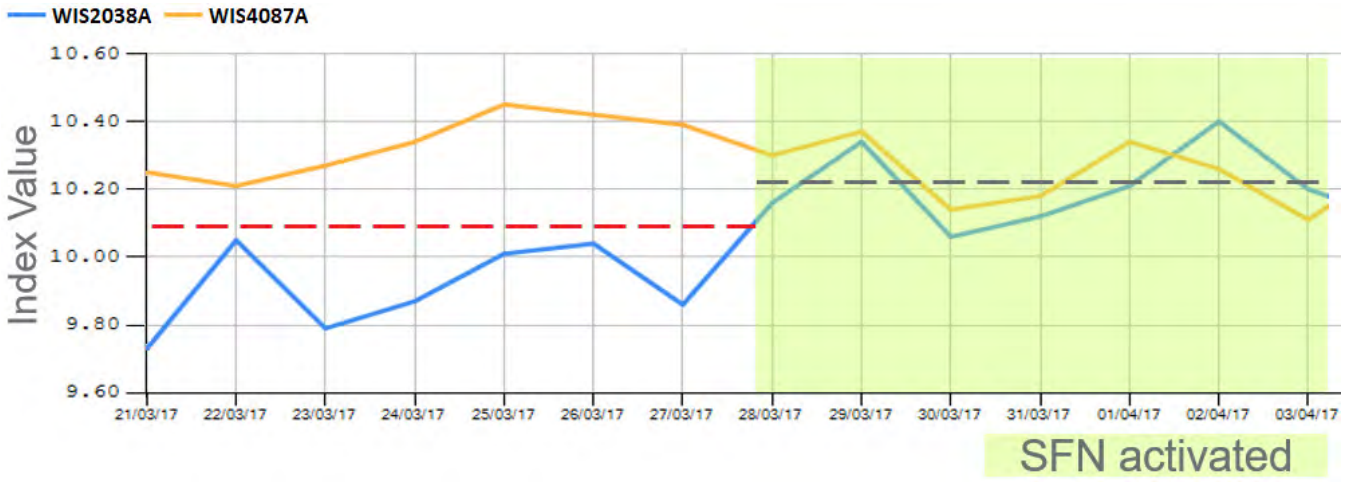

(a)

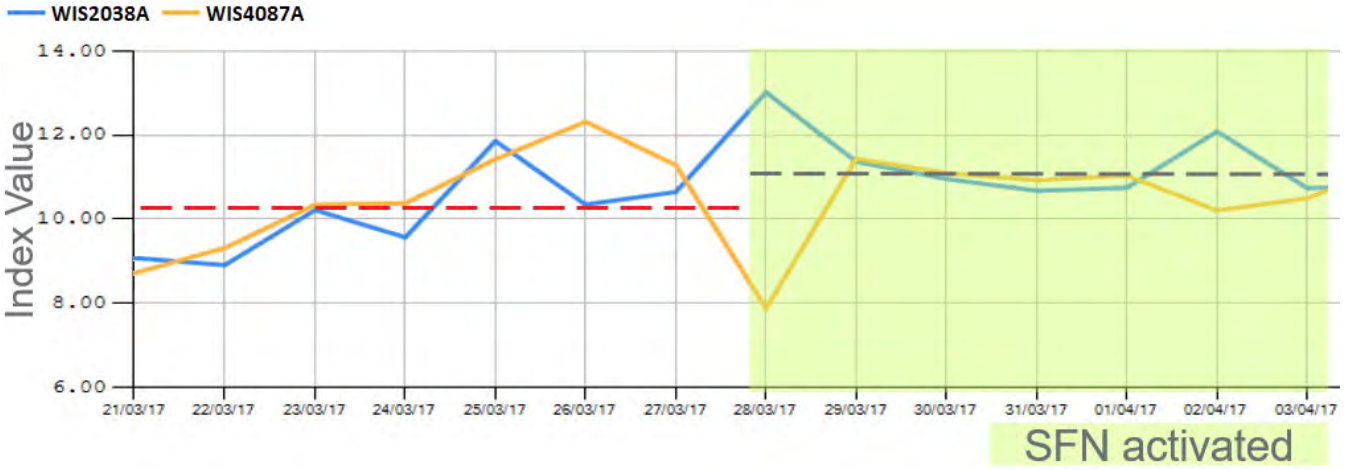

(b)

FIGURE 13. Single frequency network (a) Channel Quality Indicator (CQI). (b) Average DL MCS.

drop rates and inter/intra frequency HO out success rates. We carry out our experiments over the T = 14 days of observation duration and evaluate above KPIs by comparing before and after activation of *J-SFN based on coordinated inter-BBU* for RRU trial sites of *WIS*4087*A* and *WIS*2038*A*. Non-SFN based sites before SFN activation are selected as baseline. In both cases, performances for the individual system parameters are averaged over the corresponding observation times.

1) ACTIVE NUMBER OF USERS

In Fig. 10a, we present total number of LTE users over the observation duration. We can observe that during non-SFN and *J-SFN based on coordinated inter-BBU* activation periods, there exists instantaneous ups and downs of day-to-day subscriber numbers. However, the average number of total LTE users in a given cell over the observation period is around 300 which is same on average over both SFN and non-SFN periods. This stationary behavior of constant number of UEs represents the routine user behavior in the overlapped SFN region. This also ensures a fair comparison of SFN and non-SFN periods. Fig. 10b depicts the variation in number of jointly scheduled UEs for UL in the overlapping area during the SFN activation observation duration. Average number of jointly scheduled UEs is approximately $U = 280$. Jointly scheduled UEs receive service from both $W2038A$ and $W4087A$, which means they receive the same packet from two cells under same TTI. However, this number represents only average connected number of UEs day-to-day. In other words, not all of those UEs are actually generating UL traffic. This observation is also validated with low UL PRB utilization ratios of Fig. 11b as detailed below.

2) UL AND DL PRB UTILIZATION RATIOS

Fig. 11a and Fig. 11b depict both DL and UL PRB utilization ratios respectively for SFN active and non-SFN periods. From these figures, we observe two main results: First, during experimental SFN active observation period, low traffic load is noticed on the considered SFN cells. Second, with regard to average DL/UL PRB utilization ratios, there exists slight increase for DL PRB from 3.8% to 4.1% as shown in Fig. 11a and for UL PRB from 6.7% to 7.0% as shown in Fig. 11b when non-SFN period is compared with *J-SFN*

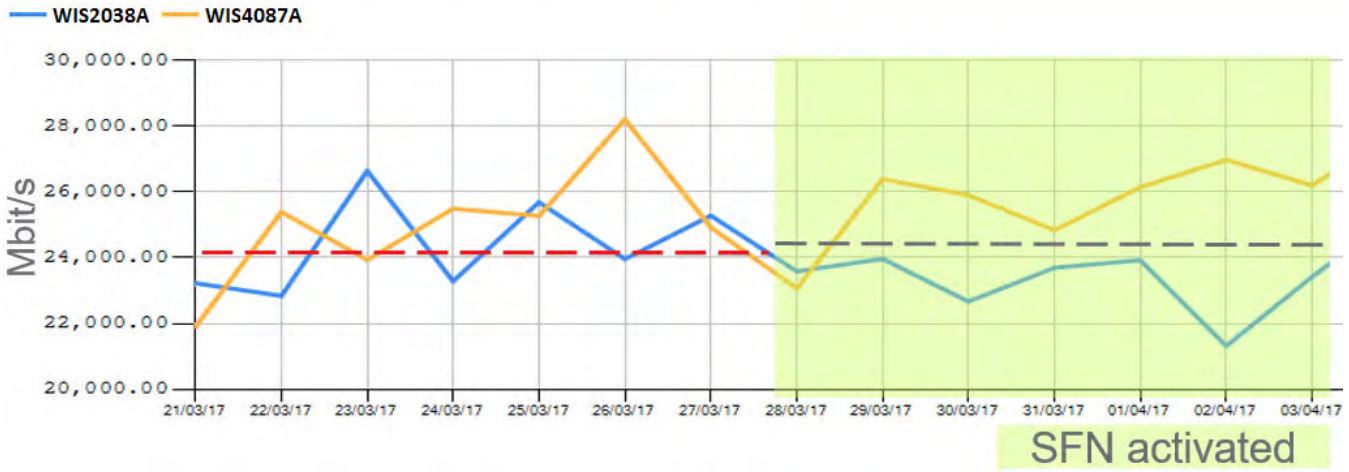

(a)

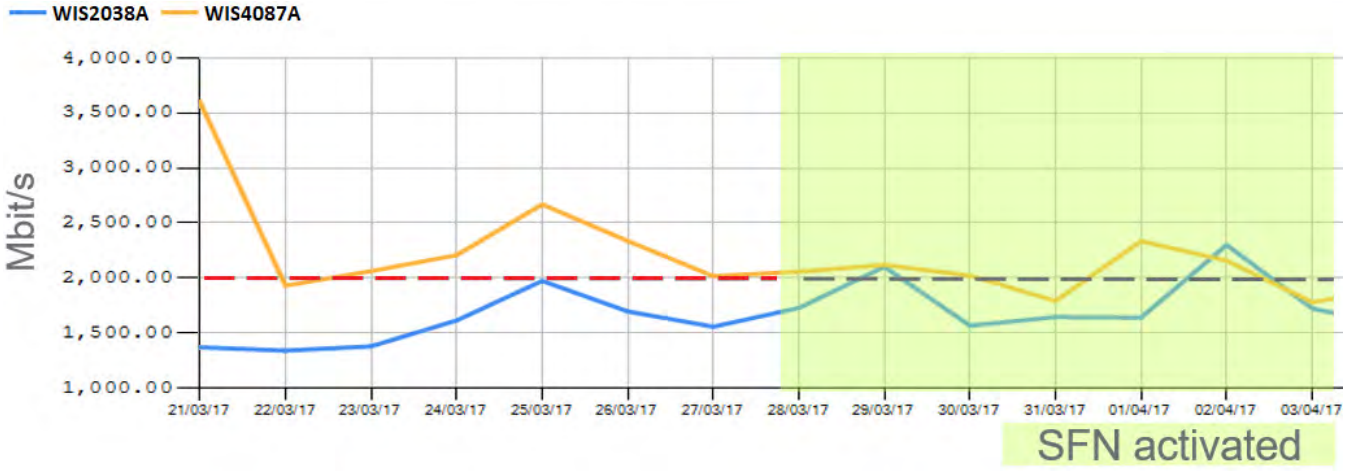

(b)

(c)

FIGURE 14. Single frequency network (a) Cell average DL throughput. (b) Cell average UL throughput. (c) DL PDCP volume.

based on coordinated inter-BBU during the observation periods. In fact, PRB utilization ratio is expected to increase with SFN feature activation due to joint scheduling process of UEs inside SFN cell. However, the main reason for small PRB utilization increase is due to low data traffic generation trends of UEs inside the overlapping SFN area. This is also observed during non-SFN periods. Hence, higher PRB utilization ratios are not observed.

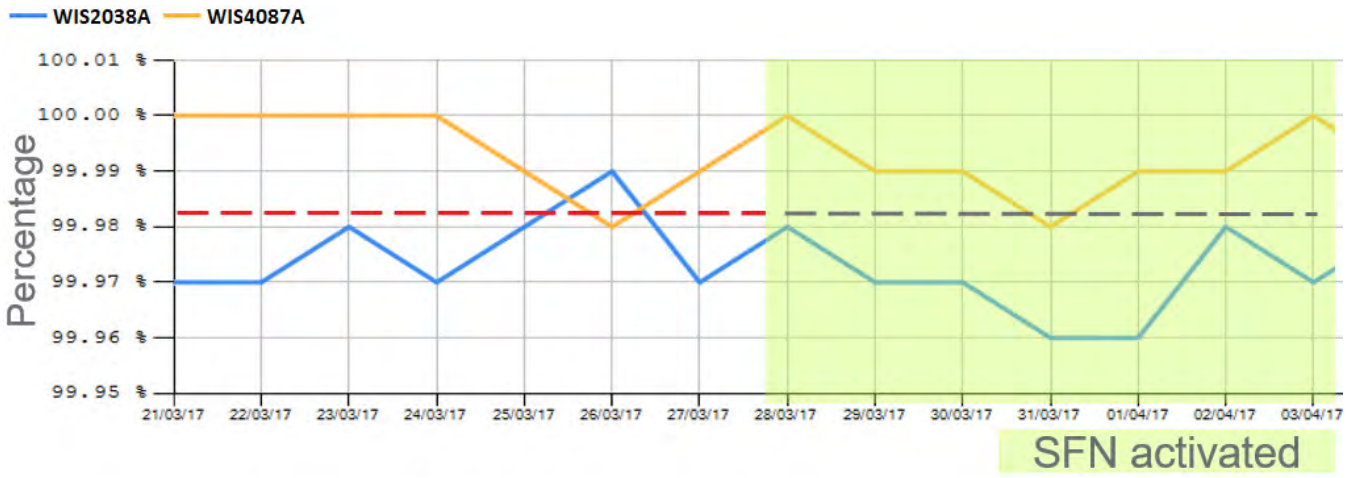

(a)

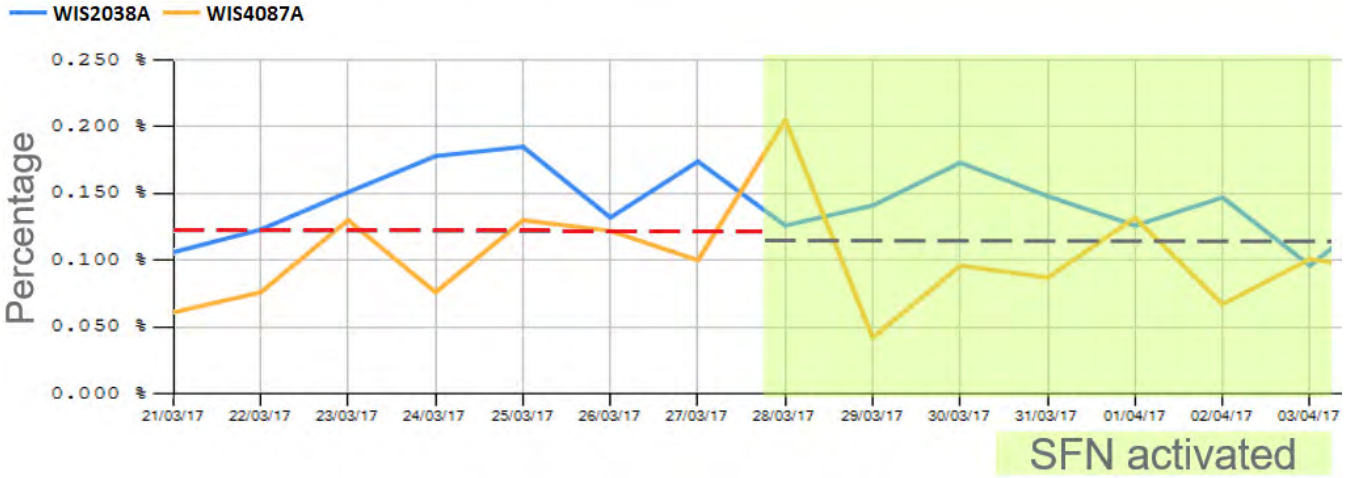

(b)

FIGURE 15. Single frequency network (a) RRC setup success rate (%). (b) Service drop rate (%).

3) CQI AND MCS VALUES

SFN is expected to provide higher SINR after appropriate cells are clustered together based on the selection process of Section V-A. To observe this fact, Fig 13 compares values of CQI and average DL MCS. *J-SFN based on coordinated inter-BBU* and non-SFN have a direct influence on both MCS and CQI values. Fig. 13a illustrates that average CQI value has improved from 10.10 to 10.21 (1.1% increase) after SFN cell is activated. Similarly in Fig. 13b, DL MCS index has improved from 10.10 to 11.30 (10.6% increase) after SFN feature is enabled. One can conclude from average DL MCS and CQI values in Fig. 13 that higher SINR (thus better connection) inside SFN cell can be achieved with the activation of SFN feature. This increase is also expected to have a positive effect on UL/DL throughput values.

4) DL AND UL THROUGHPUT

Throughput is a good representative metric to measure the system performance. Fig. 14 shows the evolution of cell average DL and UL throughput values over the observation duration. These results are observed under low network load as given in Fig. 11. In Fig. 14a, there is a slight increase in DL throughput where average DL throughput increases from 24 Gbps to 24.3 Gbps when SFN is activated. On the other hand, no major changes have occurred in UL throughput (around 2 Gbps) in comparison with non-SFN enabled observation period as given in Fig. 14b. Fig. 14c also shows slight increase in DL PDCP volume. This low increase in DL throughput and PDCP volume values is due to low data utilization trends of UEs inside the overlapping area of SFN activated region. Therefore, we can conclude that UEs inside this region continued to generate low data traffic even after SFN feature is activated.

5) RRC SET UP SUCCESS AND SERVICE DROP RATES

Fig. 15 provides illustrations of the RRC setup success rate and service drop rate percentage values over the observed duration. In general, we can notice that SFN feature activation did not have a negative effect on services provided by MNO. In Fig. 15a, RRC set-up success rates are kept

FIGURE 16. Single frequency network (a) Intra-frequency HO-out success rate (%). (b) Inter-frequency HO-out success rate (%).

constant just above 99.98%. Similarly in Fig. 15b, service drop rate percentage has decreased slightly and is around 0.12% and 0.11% before and after SFN feature action respectively. Therefore, a relatively stable service continues to be provided to UEs when SFN is activated.

6) INTER AND INTRA HO-OUT SUCCESS RATES

Fig. 16a shows the intra-frequency HO-out success rates over the observation duration for SFN cell. Intra-frequency HO-out success rate represents HOs between neighboring and SFN cell under the same EARFCN. The results indicate that with SFN cell activation, intra-frequency HO-out success rate has increased from 99.7% to 99.8%. The main reason behind this increase in success rate is due to non-existence of ping-pong HOs between cells inside SFN cell cluster. Fig. 16b depicts inter-frequency HO-out success rate over the observation duration. Inter-frequency HO represents HOs between neighboring and SFN cell with different EARFCN (e.g. between EARFCN = 1450 and EARFCN = 6200). The results indicate that inter-frequency HO-out success rate has not changed with SFN cell activation.

D. MAIN TAKEAWAYS, LESSONS LEARNED AND CHALLENGES OF SFN DEPLOYMENT

After deploying SFN feature in real operator infrastructure, it is observed that CQI and MCS values were improved. However, our experimental results did not reveal significant DL/UL throughput gains. This can be due to many reasons. One of the reasons is due to low traffic demands of end-users and as a consequence generated low traffic load inside the overlapping regions of SFN. It is noticed that PRB utilization ratios have slightly increased for UL and DL. From Fig. 14 and Fig. 11, we can observe that throughput values and PRB utilization ratios before SFN period are not so high respectively. Considering the same user behavior throughout the observation period, low data utilization in the overlapping area is noticeable. Second reason is due to the trade-off between the effects of joint Tx/Rx scheduling strategy

and large ratio of average number of jointly scheduled UEs to all LTE UEs in the considered SFN cell. In general, an increase in MCS results in lower PRB utilization ratios under constant PDCP volume due to low traffic generation trends of UEs inside SFN cell. For example, 16 QAM on 4 PRB can yield the same data volume with 64 QAM on 1 PRB for a given UE. On the other hand based on the results of Fig. 10, PRB utilization ratio is also expected to increase due to large ratio of average number of joint scheduled UEs to total number of LTE UEs. In contrast to expectations, experimental results of Fig. 11 show that when SFN cell is activated, a slight increase in PRB ratios is observed. *J-SFN based on coordinated inter-BBU* results in both throughput and PDCP volume increments, whereas large ratio of average number of jointly scheduled UEs to all LTE UEs results in large PRB utilization ratios. As a result, the effect of higher MCS's favoring small PRB utilization ratios is more pronounced during our observations. Therefore, in proportion with small increment in PRB usage ratios, small increase in throughput values of Fig. 14 is observed under constant PDCP volume. At the same time, SFN activation did not have a major impact on the services provided by MNO during live trial period where RRC set-up success rate and service drop rate values are kept relatively stable.

The main key lesson learnt from SFN deployment in real operating network is as follows: Towards designing an SFN deployment, we need to make the best choice of load percentages of RRUs. The choice of low load utilization is a dominant choice for MNOs due to expected backhaul demand of SFN after its activation. On the other hand, SFN has its own limitations as well. Implementing an SFN cell needs special care due to existence of several potential problems and challenges. First of all, achieving synchronization (temporal and frequency) between jointly scheduled cooperating cells is major issue. The transmitted signals from the transmitters are identical and should be transmitted simultaneously. Therefore, timing and frequency offsets (causing Doppler shift on received signal) together with not-identical data can break the benefits of SFN. GPS receiver connected to CSE is used for synchronization purposes in practical scenarios. Second, careful optimization and network planning requirements are needed to maximize the benefits of SFN. For example, parameters such as maximum allowed distance between two transmitters, wide or narrow transmit spacing depending on on-air redundancy and power requirements (with narrow transmitter spacing results in high on-air redundancy and high number of cooperating cells with lower transmit power and vice-versa for wide transmit spacing) can affect SFN performance. Third, in the considered *J-SFN based on coordinated inter-BBU* implementation, although a UE can be far away from other transmitters of the cells the transmission is still jointly scheduled. This can ensure transmit diversity, but at the same time RRU's effective multiplexing of traffic over their resources becomes limited.

VI. CONCLUSIONS

This paper investigates different SFN implementation scenarios using *joint scheduling in SFN based on coordinated inter-BBU* in a C-RAN experimental site. First, we studied two different SFN deployment scenarios, their benefits and limitations. Second, simulation results for non-SFN and SFN without joint scheduling were provided to observe SINR heatmap distribution over the considered experimental sites. Third, during experimental comparisons jointly scheduled SFN cell was created to observe potential performance enhancements of SFN activation period compared to non-SFN period over T = 14 days of observation duration in Cekmekoy district of Istanbul. The trials were performed on real-world live network. To benefit from SFN cell improvements maximally, a pre-trial optimization was also carried out over the experimental sites to select the cells that will cooperate during SFN deployment based on metrics such as cells with low PRB utilization ratios and higher handover attempts in between. Our experimental results demonstrated performance comparisons over extensive test cases for different KPIs including UL-DL throughput and PRB utilization ratios, DL PDCP volume, MCS, CQI, RRC set-up success/service drop rates and inter/intra-frequency HO out success rates. Our experimental results also revealed the existence of trade-off between the effect of joint transmission/reception scheduling strategy and large ratio of average number of jointly scheduled UEs to all LTE UEs in the considered SFN cell. Finally, we concluded the paper by discussing the main takeaways, lessons learned and challenges of the considered SFN implementation.

REFERENCES

[1] M. Shafi *et al.*, "5G: A tutorial overview of standards, trials, challenges, deployment, and practice," *IEEE J. Sel. Areas Commun.*, vol. 35, no. 6, pp. 1201–1221, Jun. 2017.
[2] M. J. Marcus, "5G and 'IMT for 2020 and beyond' [spectrum policy and regulatory issues]," *IEEE Wireless Commun.*, vol. 22, no. 4, pp. 2–3, Aug. 2015.
[3] 5G Americas. (Aug. 2018). *LTE to 5G: The Global Impact of Wireless Innovation*. Accessed: Aug. 21, 2018. [Online]. Available: http://www.5gamericas.org/files/4915/3479/4684/2018_5G_Americas_Rysavy_LTE_to_5G-_The_Global_Impact_of_Wireless_Innovation_final.pdf
[4] L. Dong *et al.*, "Introduction on IMT-2020 5G trials in China," *IEEE J. Sel. Areas Commun.*, vol. 35, no. 8, pp. 1849–1866, 2017.
[5] M. Pätzold, "5G developments are in full swing [mobile radio]," *IEEE Veh. Technol. Mag.*, vol. 12, no. 2, pp. 4–12, Jun. 2017.
[6] International Telecommunication Union (ITU). (2018). *Setting the Scene for 5G: Opportunities & Challenges*. Accessed: Sep. 23, 2018. [Online]. Available: http://itu.int/en/ITU-D/Documents/ITU_5G_REPORT-2018.pdf
[7] V. W. S. Wong, R. Schober, D. W. K. Ng, and L.-C. Wang, "Overview of new technologies for 5G systems," in *Key Technologies for 5G Wireless Systems*. Cambridge, U.K.: Cambridge Univ. Press, 2017, p. 1.
[8] Y. Liu, W. Li, H. Zhang, and L. Yu, "Distributed PCI assignment in LTE based on consultation mechanism," in *Proc. 6th Int. Conf. Wireless Commun. Netw. Mobile Comput. (WiCOM)*, Sep. 2010, pp. 1–4.
[9] R. Sivaraj, M. Arslan, K. Sundaresan, S. Rangarajan, and P. Mohapatra, "BoLTE: Efficient network-wide LTE broadcasting," in *Proc. IEEE 25th Int. Conf. Netw. Protocols (ICNP)*, Oct. 2017, pp. 1–10.
[10] A. Daher, M. Coupechoux, P. Godlewski, P. Ngouat, and P. Minot, "SC-PTM or MBSFN for mission critical communications?" in *Proc. IEEE 85th Veh. Technol. Conf. (VTC Spring)*, Jun. 2017, pp. 1–6.

[11] C. Borgiattino, C. Casetti, C.-F. Chiasserini, and F. Malandrino, "Efficient area formation for LTE broadcasting," in *Proc. SECON*, 2015, pp. 202–210.
[12] F. Rinaldi, P. Scopelliti, A. Iera, A. Molinaro, and G. Araniti, "Delivering multimedia services in MBSFN areas over 5G networks: A performance analysis," in *Proc. IEEE Int. Symp. Broadband Multimedia Syst. Broadcast. (BMSB)*, Jun. 2018, pp. 1–5.
[13] G. Araniti, M. Condoluci, P. Scopelliti, A. Molinaro, and A. Iera, "Multicasting over emerging 5G networks: Challenges and perspectives," *IEEE Netw.*, vol. 31, no. 2, pp. 80–89, Mar./Apr. 2017.
[14] J. Montalban *et al.*, "Multimedia multicast services in 5G networks: Subgrouping and non-orthogonal multiple access techniques," *IEEE Commun. Mag.*, vol. 56, no. 3, pp. 91–95, Mar. 2018.
[15] F. B. Tesema, A. Awada, I. Viering, M. Simsek, and G. P. Fettweis, "Multiconnectivity for mobility robustness in standalone 5G ultra dense networks with intrafrequency cloud radio access," *Wireless Commun. Mobile Comput.*, vol. 2017, Jan. 2017, Art. no. 2038078.
[16] A. Prasad, P. Lunden, Z. Li, and M. A. Uusitalo, "Enhancements for enabling point-to-multipoint communication using unlicensed spectrum," in *Proc. IEEE Int. Symp. Broadband Multimedia Syst. Broadcast. (BMSB)*, Jun. 2018, pp. 1–5.
[17] T. Takada, K. Teshima, and H. Harada, "Performance enhancement technologies in high-speed moving mobile environment in LTE-advanced release 14," *NTT Docomo Tech. J.*, vol. 9, no. 3, pp. 64–70, 2018. Accessed: Sep. 25, 2018.
[18] *Study on Performance Enhancements for High Speed Scenario in LTE*, document 3GPP TR 36.878, 2016.
[19] "Cloud RAN architecture for 5G," Telefónica-Ericsson, White Paper, 2015. [Online]. Available: https://goo.gl/KodmmT
[20] O. D. Ramos-Cantor, J. Belschner, G. Hegde, and M. Pesavento, "Centralized coordinated scheduling in LTE-advanced networks," *EURASIP J. Wireless Commun. Netw.*, vol. 2017, no. 1, p. 122, 2017.
[21] G. Nardini *et al.*, "Practical feasibility, scalability and effectiveness of coordinated scheduling algorithms in cellular networks towards 5G," *J. Netw. Comput. Appl.*, vol. 106, pp. 1–16, Mar. 2018.
[22] M. Awais *et al.*, "Efficient joint user association and resource allocation for cloud radio access networks," *IEEE Access*, vol. 5, pp. 1439–1448, 2017.
[23] O. Narmanlioglu and E. Zeydan, "New era in shared cellular networks: Moving into open and virtualized platform," *Int. J. Netw. Manage.*, vol. 27, no. 6, p. e1986, 2017.
[24] A. Douik, H. Dahrouj, T. Y. Al-Naffouri, and M.-S. Alouini, "Coordinated scheduling for the downlink of cloud radio-access networks," in *Proc. IEEE Int. Conf. Commun. (ICC)*, Jun. 2015, pp. 2906–2911.
[25] C.-L. I, J. Huang, R. Duan, C. Cui, J. Jiang, and L. Li, "Recent progress on C-RAN centralization and cloudification," *IEEE Access*, vol. 2, pp. 1030–1039, 2014.
[26] A. Checko *et al.*, "Cloud RAN for mobile networks: A technology overview," *IEEE Commun. Surveys Tuts.*, vol. 17, no. 1, pp. 405–426, 1st Quart., 2015.
[27] "C-RAN: The road towards green RAN," China Mobile, Beijing, China, White Paper ver. 2.5, 2011, pp. 1–10.
[28] M. Peng, Y. Sun, X. Li, Z. Mao, and C. Wang, "Recent advances in cloud radio access networks: System architectures, key techniques, and open issues," *IEEE Commun. Surveys Tuts.*, vol. 18, no. 3, pp. 2282–2308, 3rd Quart., 2016.
[29] O. Narmanlioglu and E. Zeydan, "Interference coordination in SDN-based heterogeneous mobile networks," in *Proc. IEEE Int. Black Sea Conf. Commun. Netw. (BlackSeaCom)*, Jun. 2017, pp. 1–6.
[30] Y. Kakishima, T. Kawamura, Y. Kishiyama, H. Taoka, and T. Nakamura, "Experimental evaluation on throughput performance of asymmetric carrier aggregation in LTE-Advanced," in *Proc. IEEE 73rd Veh. Technol. Conf. (VTC Spring)*, May 2011, pp. 1–5.
[31] Z. Kaleem and K. Chang, "QoS priority-based coordinated scheduling and hybrid spectrum access for femtocells in dense cooperative 5G cellular networks," *Trans. Emerg. Telecommun. Technol.*, vol. 29, no. 1, p. e3207, 2018.
[32] A. Davydov, G. Morozov, I. Bolotin, and A. Papathanassiou, "Evaluation of joint transmission CoMP in C-RAN based LTE-A HetNets with large coordination areas," in *Proc. IEEE Globecom Workshops (GC Wkshps)*, Dec. 2013, pp. 801–806.
[33] S. Ali and M. Synthia, "Performance analysis of JT-CoMP transmission in heterogeneous network over unreliable backhaul," in *Proc. Int. Conf. Elect. Eng. Inf. Commun. Technol. (ICEEICT)*, 2015, pp. 1–5.
[34] A. Nagate, S. Nabatame, D. Ogata, K. Hoshino, and T. Fujii, "Field experiment of CoMP joint transmission over X2 interface for LTE-advanced," in *Proc. IEEE 77th Veh. Technol. Conf. (VTC Spring)*, 2013, pp. 1–5.
[35] *Coordinated Multi-Point Operation for LTE Physical Layer Aspects (Release 11)*, document 3GPP TR 36.819, 2013.
[36] S. I. Popoola, A. A. Atayero, N. Faruk, C. T. Calafate, L. A. Olawoyin, and V. O. Matthews, "Standard propagation model tuning for path loss predictions in built-up environments," in *Computational Science and Its Applications—ICCSA* (Lecture Notes in Computer Science), vol. 10409, O. Gervasi *et al.*, Eds. Cham, Switzerland: Springer, 2017.
[37] Atoll. (2018). *Atoll Radio Planning Software*. Accessed: Oct. 25, 2018. [Online]. Available: http://www.forsk.com/atoll-overview
[38] A. S. Abdulrasool, J. S. Aziz, and S. J. Abou-Loukh, "Calculation algorithm for diffraction losses of multiple obstacles based on Epstein–Peterson approach," *Int. J. Antennas Propag.*, vol. 2017, Oct. 2017, Art. no. 3932487.

YEKTA TURK received the B.Sc. degree in electrics and electronics engineering from Anadolu University, Turkey, in 2005, the M.Sc. degree in telecommunications and computer networks from The George Washington University, DC, USA, in 2007, and the Ph.D. degree from the Department of Computer Engineering, Maltepe University, Istanbul, Turkey, in 2018. He worked with a Fixed and Mobile Network Operator for 10 years. He is currently a Senior Engineer with the Mobile Access System Architecture Department, Turk Telekom, Turkey. His research interests include mobile radio telecommunications and wireless sensor networks.

ENGIN ZEYDAN received the B.Sc. and M.Sc. degrees from the Department of Electrical and Electronics Engineering, Middle East Technical University, Ankara, Turkey, in 2004 and 2006, respectively, and the Ph.D. degree from the Department of Electrical and Computer Engineering, Stevens Institute of Technology, Hoboken, NJ, USA, in 2011. He was a Research and Development Engineer with Avea, a mobile operator in Turkey, between 2011 and 2016. He was a Senior Research and Development Engineer with Turk Telekom Labs, between 2016 and 2018. He was also a Part-Time Instructor with the Electrical and Electronics Engineering Department, Ozyegin University, from 2015 to 2018. He is currently a Researcher with the Communication Networks Division, Centre Tecnologic de Telecomunicacions de Catalunya. His research interests include telecommunications and big data networking. He received the Best Paper Award from the Network of Future Conference, in 2017.

CEMAL ALP AKBULUT received the B.Sc. and M.Sc. degrees from the Department of Electronics and Communication Engineering, Istanbul Technical University, Istanbul, Turkey, in 1991 and 1995, respectively. In 1996, he started his professional career as a Research and Development Analog Circuit Design Engineer for four months. He was a Support Engineer for narrow band and spread spectrum wireless handheld terminals, until 1999. He participated in local and overseas radio network optimization projects as an Engineer, a Senior Engineer, a Team Manager, a Project Manager, and a Project Mentor, until 2011. He was a Radio Network Optimization Expert with Avea, Mobile Operator in Turkey, between 2011 and 2016. Since 2000, he has been with Alcatel Teletas, where he focuses on 3GPP-based mobile technologies. He is currently an Expert Engineer with the Mobile Access Architecture Department, Turk Telekom. His research interests include mobile radio telecommunications and next-generation mobile networks.